Earth's Future

RESEARCH ARTICLE
10.1029/2019EF001331

Global Socioeconomic Risk of Precipitation Extremes Under Climate Change

Yujie Liu[1,2], Jie Chen[1,2], Tao Pan[1], Yanhua Liu[1,2], Yuhu Zhang[3], Quansheng Ge[1,2], Philippe Ciais[4], and Josep Penuelas[5,6]

[1]Key Laboratory of Land Surface Pattern and Simulation, Institute of Geographic Sciences and Natural Resources Research, Chinese Academy of Sciences (CAS), Beijing, China, [2]University of Chinese Academy of Sciences (UCAS), Beijing, China, [3]Capital Normal University, Beijing, China, [4]Laboratoire des Sciences du Climat et de l'Environnement, IPSL-LSCE CEA CNRS UVSQ, Gif-sur-Yvette, France, [5]CSIC, Global Ecology CREAF-CSIC-UAB, Barcelona, Catalonia, Spain, [6]CREAF, Barcelona, Catalonia, Spain

Key Points:
- Global population and GDP exposures are highest for 2046–2065 in RCP8.5-SSP3 and RCP2.6-SSP1, 8.46×10^{10} person-days and 2.29×10^{15}PPP $-days
- Increases in population and GDP are the dominant contributors, accounting for over 60% of future changes in socioeconomic exposure
- Effective adaptation is urgently needed for some European countries, for example, Luxembourg, the Netherlands, and Belgium, and in Asia and Africa

Supporting Information:
- Supporting Information S1

Correspondence to:
Y. Liu, T. Pan, and Q. Ge,
liuyujie@igsnrr.ac.cn;
pantao@igsnrr.ac.cn;
geqs@igsnrr.ac.cn

Citation:
Liu, Y., Chen, J., Pan, T., Liu, Y., Zhang, Y., Ge, Q., et al. (2020). Global socioeconomic risk of precipitation extremes under climate change. *Earth's Future*, *7*, e2019EF001331. https://doi.org/10.1029/2019EF001331

Received 25 JUL 2019
Accepted 4 AUG 2020
Accepted article online 10 AUG 2020

Abstract Precipitation extremes are among the most serious consequences of climate change around the world. The observed and projected frequency and intensity of extreme precipitation in some regions will greatly influence the social economy. The frequency of extreme precipitation and the population and economic exposure were quantified for a base period (1986–2005) and future periods (2016–2035 and 2046–2065) based on bias corrected projections of daily precipitation from five global climatic models forced with three representative concentration pathways (RCPs) and projections of population and gross domestic product (GDP) in the shared socioeconomic pathways (SSPs). The RCP8.5-SSP3 scenario produces the highest global population exposure for 2046–2065, with nearly 30% of the global population (2.97×10^9 persons) exposed to precipitation extremes >10 days/a. The RCP2.6-SSP1 scenario produces the highest global GDP exposure for 2046–2065, with a 5.56-fold increase relative to the base period, of up to $(2.29 \pm 0.20) \times 10^{15}$ purchasing power parity $-days. Socioeconomic effects are the primary contributor to the exposure changes at the global and continental scales. Population and GDP effects account for 64–77% and 78–91% of the total exposure change, respectively. The inequality of exposure indicates that more attention should be given to Asia and Africa due to their rapid increases in population and GDP. However, due to their dense populations and high GDPs, European countries, that is, Luxembourg, Belgium, and the Netherlands, should also commit to effective adaptation measures.

Plain Language Summary The risk of precipitation extremes is likely to increase with climate change. Socioeconomic exposure is the key component for assessing the risk of such events. The projections of five global climate models (GCMs), forced with three representative concentration pathways (RCPs) and projections of population and gross domestic product (GDP) in shared socioeconomic pathways (SSPs), were used to quantify socioeconomic exposure to precipitation extremes for a base period (1986–2005) and future periods (2016–2035 and 2046–2065). The exposure of the global population for 2046–2065 is highest under the RCP8.5-SSP3 scenario, and the global GDP exposure for 2046–2065 is highest under the RCP2.6-SSP1 scenario. Socioeconomic effects (population and GDP effects) play the main roles in the changes in exposure at both global and continental scales. Asia and Africa should be given more attention due to their rapid increases in population and GDP. However, due to their dense populations and high GDPs, European countries should also commit to effective adaptation measures.

1. Introduction

There is increasing evidence that the global temperature has continued to rise due to human activity such as the industrial, transport and other sectors in the past decades. A changing climate leads to changes in the frequency, intensity, spatial extent, duration, and timing of climate extremes (IPCC, 2013). A climate extreme is the occurrence of a value of a weather or climate variable above (or below) a threshold value near the upper (or lower) end of the range of observed values of the variable. Both extreme weather events and extreme climate events are referred to collectively as "climate extremes" and include extreme precipitation, extreme temperatures, and drought (IPCC, 2012; WMO, 2010). The global mean temperature for 2019 was 1.1 ± 0.1°C above preindustrial levels (1850–1900) (WMO, 2020). Surface evaporation

and the airborne water content have also increased, increasing the intensity of global and regional water cycles and the probability of extreme precipitation (Giorgi et al., 2011; Liu et al., 2015). As one of the most widespread types of natural disaster especially in rainy regions, extreme precipitation has a large impact on people's lives, property, and the environment (Bowles et al., 2014; IPCC, 2014; Min et al., 2011). Anticipating changes in extreme precipitation and its impact on the social economy under climate change is therefore critical and would help to provide a scientific basis for disaster prevention and reduction.

The frequency and intensity of extreme precipitation are likely to increase during this century (Kharin et al., 2013; Westra et al., 2014). This is expected to affect many people and the gross domestic product (GDP) of many countries, as well as increasing the disaster risk globally (Carleton & Hsiang, 2016; Ceola et al., 2015). The risk of a disaster occurs due to the interaction of hazard, exposure, and vulnerability, among which exposure usually refers to the presence of people, livelihoods, species or ecosystems, environmental functions, services, resources, infrastructure, or economic, social, and cultural assets in places and settings that could be adversely affected (IPCC, 2014). Estimating spatiotemporal variation and changes in exposure to extreme precipitation is therefore a key procedure in quantifying future vulnerability and risk (King et al., 2018; Pryor et al., 2014; Smirnov et al., 2016).

Many previous studies have projected the future hazard of climate extremes under climate change. For example, Toreti et al. (2013) provided new projected global precipitation extremes for the 21st century, with a significant intensification of daily extremes projected for the middle and high latitudes of both hemispheres at the end of the present century. Cook et al. (2015) estimated global drying and wetting trends in the 21st century using two drought indices and found that increases in potential evapotranspiration due to global warming would have additional impacts through regional drying. In addition to the change in frequency and intensity of climate extremes, the severity of the impacts of these extremes is largely determined by socioeconomic exposure and vulnerability to these climate extremes. However, our understanding of the socioeconomic impact of climate extremes at the global scale in a warmer climate is limited. Therefore, a robust characterization of socioeconomic exposure to future extreme precipitation is important for effective mitigation and adaptation strategies.

Several attempts have been made to estimate the future regional socioeconomic impacts of extreme precipitation. For example, Houser et al. (2015) and Hsiang et al. (2017) quantified economic losses under climate change in America. Forzieri et al. (2017) assessed the impacts of weather-related hazards, including extreme precipitation, on the European population in terms of the annual number of deaths. However, there is limited evidence indicating how socioeconomic exposure to extreme precipitation would impact society at a global scale (Bouwer, 2013). Most previous studies have quantified future exposure and risk using fixed estimates of population and GDP; for example, population exposure has been calculated by the frequency of climate extremes in future scenarios multiplied by the current population data (Sun et al., 2017), with no consideration of changes in socioeconomic factors. This is not sufficient for projecting changes in exposure, because both climate change and socioeconomic change are key factors affecting exposure. Additionally, population and GDP exposures are usually projected separately and are rarely used to assess socioeconomic exposure together, even though the spatial distributions of populations and economies are consistent. Some studies have focused on specific increases in global mean temperature (GMT) (King et al., 2017; Mitchell et al., 2017; Zhang et al., 2018). Projecting changes in future impacts associated with climate warming in different climate scenarios and time periods is challenging. In particular, little is known about the areas with the highest exposure to extreme precipitation, where effective adaptation measures are urgently needed to address climate change.

The primary goal of this study is to quantify the global spatiotemporal distribution and changes in exposure of population and GDP to extreme precipitation under different scenarios and over different time periods. Additionally, the impact of climate change, population and GDP effects, and the interaction effect was estimated. Furthermore, the inequality of population and GDP exposures among countries was quantified. Based on these analyses, we characterized the future spatiotemporal distribution and increase in socioeconomic exposure to extreme precipitation and clarified the relative importance of future changes in exposure, as well as identifying regions where the design and implementation of effective measures of adaptation are needed.

2. Materials and Methods

2.1. Data

Simulation results were obtained using the representative concentration pathways (RCPs, Vuuren, Edmonds, Kainuma, Riahi, Thomson, et al., 2011) from the Coupled Model Intercomparison Project Phase 5 (CMIP5, Taylor et al., 2012). Simulations were based on projections of daily precipitation from the Inter-Sectoral Impact Model Intercomparison Project (ISI-MIP, Warszawski et al., 2014), which contains five global climate models (GCMs, Table S1 in the supporting information). The output data were spatially downscaled by being bi-linearly interpolated to 0.5° × 0.5° resolution (Warszawski et al., 2014). Wherever necessary, the time series were linearly interpolated to the standard Gregorian calendar, that is, 365 days/year plus the leap day (Hempel et al., 2013). A statistical bias correction facilitated the comparison of observed and simulated impacts during the historical reference period and enabled a continuous transition into the future (Hempel et al., 2013). The preservation of absolute changes in monthly temperature, and relative changes in monthly values of precipitation in each grid cell implied the global warming trend. The climate sensitivities of the GCMs were preserved, and the trend and the long-term mean were well represented, which ensured the credibility of the simulated data (Warszawski et al., 2014).

Some organizations, such as the United Nations and World Bank, have proposed socioeconomic projections, while many of these organizations do not consider population and GDP changes in different scenarios under climate change. In this study, population and GDP projections in the shared socioeconomic pathways (SSPs) corresponding to the RCPs were obtained from the National Institute for Environmental Studies, Japan (NIES) (Murakami & Yamagata, 2019), which were downscaled from the International Institute for Applied Systems Analysis (IIASA). The spatial resolution is 0.5° × 0.5° for latitude and longitude. The RCPs are based on the simulated impacts of land use, aerosols, and greenhouse-gas (GHG) emissions. The four RCPs extend to 2,100, with published values of radiative forcing ranging from 2.6 to 8.5 W/m^2 (Vuuren, Edmonds, Kainuma, Riahi, & Weyant, 2011). The SSPs are reference pathways that describe plausible alternative trends in the evolution of society and ecosystems over a century independently with climate change or climate policies. SSP1, SSP2, and SSP3 denote low, intermediate, and high challenges, respectively; SSP4 and SSP5 are dominated by adaptation challenges and mitigation challenges, respectively (O'Neill et al., 2014). Based on the four RCP scenarios and five SSP scenarios, a 4 × 5 matrix could be generated by combining climate data in the RCPs and socioeconomic data in the SSPs (Van Vuuren & Carter, 2014). However, some RCP-SSP combinations (e.g., RCP8.5-SSP1) are unlikely to arise in practice. Therefore, three combinations that are most consistent and have been mostly widely used previously were selected for analysis in this study (i.e., RCP2.6-SSP1, RCP4.5-SSP2, and RCP8.5-SSP3) (IPCC, 2014; Liu et al., 2017; O'Neill et al., 2017). Among the three combinations (Table 1), the RCP2.6-SSP1 scenario represents low carbon emissions, with sustainable development proceeding at a reasonably high pace and inequalities being lessened. The RCP4.5-SSP2 scenario indicates moderate carbon emissions, with moderate growth of the population and economy. The RCP8.5-SSP3 scenario indicates high carbon emissions, with a rapidly growing population and low adaptive capacity (O'Neill et al., 2017). Among the three SSPs, population projections are highest in SSP3, followed by SSP2 and SSP1, while the fastest GDP growth occurs in SSP1, followed by SSP2, and SSP3.

2.2. Methods

2.2.1. Frequency of extreme precipitation

The measure of hazard used in this study was the annual number of days of extreme precipitation, which also expresses the frequency of extreme precipitation. The definition of extreme precipitation is daily precipitation exceeding a given threshold. The common indices used for extreme precipitation include absolute and relative thresholds. The indices of extreme precipitation used in early studies typically had an absolute threshold, with a fixed value in a particular study area (Groisman et al., 1999). However, the hazard of extreme events depends on the physical characteristics of the event, the geographical environment, infrastructure, and awareness of the residents. For example, a small amount of precipitation in arid and semi-arid regions may cause floods and landslides, and therefore, an absolute threshold in such areas cannot adequately indicate the hazard of extreme precipitation. We therefore used a relative threshold, defined as the 95th percentile of wet days (with precipitation >1 mm) over the base period (1986–2005). Compared to an absolute threshold, a relative threshold, which fully considers the regional differences in

Table 1
Combination of Representative Concentration Pathways (RCPs) and Shared Socioeconomic Pathways (SSPs) and the Characteristics of Different RCP-SSP Scenarios

Representative concentration pathways (RCPs)	Shared socioeconomic pathways (SSPs)		
	SSP1 (sustainability)	SSP2 (middle of the road)	SSP3 (regional rivalry)
RCP2.6	√ Low challenge for adaptation, High challenge for mitigation		
RCP4.5		√ Medium challenge for adaptation and mitigation	
RCP8.5			√ High challenge for adaptation Low challenge for mitigation

precipitation, eliminates regional and seasonal factors and determines the thresholds of extreme precipitation in various locations based on the actual precipitation conditions in each location. This is more suitable for projecting spatiotemporal variation and changes in exposure globally due to the large differences in climatic conditions around the world (Liu et al., 2017). In this study, the results of five GCMs were synthesized based on the separately calculated frequency and exposure for each GCM. The frequency of extreme precipitation was calculated as follows:

$$C = \sum_{i=1}^{365} (PRE_i > THR), \tag{1}$$

$$\overline{C} = \frac{\sum_{j=1}^{5} C_j}{5}, \tag{2}$$

$$\sigma = \sqrt{\frac{1}{5} \sum_{j=1}^{5} (C_j - \overline{C})}, \tag{3}$$

where C is the annual number of days of extreme precipitation (day), i is the ith day of a year, PRE is the daily precipitation (mm), THR is the local threshold (mm), $\overline{C}$ is the multimodel averaged value of C (day), j is the jth GCM, and σ is the standard deviation of C, which indicates the multimodel uncertainty.

2.2.2. Population and GDP exposure to extreme precipitation

The definition of demographic and economic exposure is the number of days with extreme precipitation multiplied by the number of people and amount of GDP exposed to that outcome in each grid cell (Jones et al., 2015). The units are person-days for population exposure and purchasing-power parity (PPP, dollar-days) for GDP exposure. Twenty-year averages of annual days of extreme precipitation and population and GDP projections were used to calculate exposure in both the base and future periods to minimize inter-annual variations. A 20-year mean exposure was calculated for each grid cell and was aggregated to global, continental, and national scales.

$$\overline{E_P} = \frac{\sum_{m=1}^{20} C_m \times P}{20}, \tag{4}$$

$$\overline{E_G} = \frac{\sum_{m=1}^{20} C_m \times G}{20}, \tag{5}$$

where $\overline{E_P}$ is the 20-year averaged population exposure (person-day), m is the mth year of the study period, C is the annual days of extreme precipitation (day), P is the population simulation (person), $\overline{E_G}$ is the 20-year averaged GDP exposure (PPP dollar-days), and G is the GDP simulation (PPP dollar).

2.2.3. Analysis of the relative importance of changes in exposure

Changes in population and GDP exposure were decomposed into the effects of climate, population/GDP, and their interactions to clarify the contribution of climate and socioeconomic factors to changes in exposure, using previously reported techniques (Jones et al., 2015). The impact of socioeconomic factors (population/GDP) was calculated by holding climate constant, that is, using the 20-year average of annual days of extreme precipitation in the base period multiplied by the population/GDP in the RCP-SSP scenarios. The population/GDP was similarly held constant when calculating the impact of climate, that is, the 20-year

average of annual days of extreme precipitation in the RCP scenarios was multiplied by the population in the base period. The interactive effects were also evaluated to assess whether the areas with continued population/GDP growth had more extreme precipitation under climate change. The changes in population and GDP exposure were decomposed using Equations 1 and 2, respectively:

$$\Delta E_P = C_b \times \Delta P + P_b \times \Delta C + \Delta P \times \Delta C, \tag{6}$$

$$\Delta E_G = C_b \times \Delta G + G_b \times \Delta C + \Delta G \times \Delta C, \tag{7}$$

where ΔE_P is the total change in population exposure (person-day), C_b is the annual days of extreme precipitation in the base period (day), ΔP is the change in population (person), P_b is the population in the base period (person), ΔC is the change in annual days of extreme precipitation from the base period to the future period (day), ΔE_G is the total change in GDP exposure (PPP dollar-days), ΔG is the change in GDP (PPP dollar), and G_b is GDP in the base period (PPP dollar). Therefore, $C_b \times \Delta P$ is the population effect, $C_b \times \Delta G$ is the GDP effect, $P_b \times \Delta C$ and $G_b \times \Delta C$ are the climatic effects, and $\Delta P \times \Delta C$ and $\Delta G \times \Delta C$ are the interactive effects between climate change and socioeconomic change (i.e., population and GDP change).

3. Results

3.1. Spatial distribution and change of extreme precipitation frequency

The spatial distribution of extreme precipitation frequency is heterogeneous in each time period and scenario (Figure S1). Extreme precipitation events occur most frequently in regions with a wet tropical climate near the equator, most of which have >15 annual average days of extreme precipitation. Extreme precipitation is also frequent in monsoon areas, such as eastern, southern, and southeastern Asia; southern and southeastern North America; and eastern and southern South America. The average frequency of extreme precipitation for the five GCMs is projected to increase with global warming. The frequency in the RCP scenarios increases relative to the base period, with the increase under the same scenario being more pronounced for 2046–2065 than 2016–2035. The frequency is highest in RCP 8.5, followed by RCP 4.5 and RCP 2.6. The change of extreme precipitation frequency is spatially variable, with rapid increases in western and northern Europe in the future RCP scenarios. In addition to the internal variability of the climate system, the long-term changes in the frequency of extreme precipitation are dominated by the impact of climate change.

3.2. Spatiotemporal patterns and changes of population and GDP exposure to extreme precipitation

The global spatial distribution of population and GDP exposures are similar under the various scenarios and time periods. The spatial distribution of results with the highest population and GDP exposures scenarios are shown in Figure 1, and the spatial patterns for the other scenarios are shown in Figure S2. Regions with a higher exposure to extreme precipitation are mainly located in densely populated areas. Exposure is larger for 2046–2065 than 2016–2035 under the same scenario, which is due to the growth of population and GDP over time combined with the increase in extreme precipitation (Tables S2 and S3). Exposure is also much higher under the RCP scenarios than in the base period. For example, global annual population exposure in the base period is $(4.34 \pm 0.34) \times 10^{10}$ person-days, which increases to $(8.46 \pm 0.74) \times 10^{10}$ person-days for 2046–2065 under the RCP8.5-SSP3 scenario, representing a 1.95-fold increase relative to the base period (i.e., the scenario and time period with the largest population increase, a 1.62-fold increase compared to the base period). The GDP exposure increases to $(2.29 \pm 0.20) \times 10^{15}$ PPP dollar-days for 2046–2065 under the RCP2.6-SSP1 scenario, representing a 6.56-fold increase relative to the base period (i.e., the scenario and time period with the largest GDP increase had a 5.02-fold increase in exposure compared to the base period).

We also estimated the population exposed to extreme precipitation on more than 10 days per year, because the impact on individuals varied depending on whether they are exposed to one or several extreme precipitation events. In the base period, there are 8.19×10^8 persons exposed to extreme precipitation on more than 10 days per year, which accounts for 13% of the global population in that period. During 2046–2065, under the RCP8.5-SSP3 scenario, the population exposed to extreme precipitation on more than 10 days per year

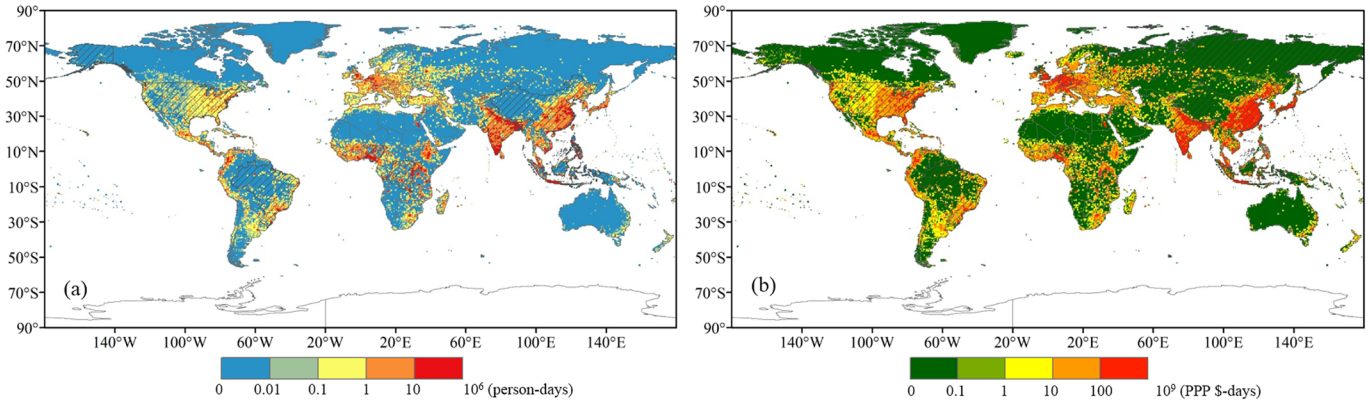

Figure 1. Spatial distribution for 2046–2065 of (a) population exposure in the RCP8.5-SSP3 scenario and (b) GDP exposure in the RCP2.6-SSP1 scenario, as projected by multimodel averages. The 10 countries with the highest exposures are highlighted as diagonal lines. PPP refers to purchasing-power parity and $ refers to US dollars.

increases to 2.97×10^9 persons, which represents nearly 30% of the global population in that scenario. Continental population exposure is highest for Asia, followed by Africa. Oceania has the lowest exposure in both the base period and under the RCP scenarios (Table S2), while Asia accounts for nearly 50% of the global population exposure under each scenario. The GDP exposure is high in eastern and southern Asia, western Europe, eastern North America, southeastern South America, and central Africa (Figure 1b). Continental GDP exposure for 2046–2065 in RCP2.6-SSP1 follows the order of Asia > Europe > North America > Africa > South America > Oceania.

The relative changes in population exposure under the projected scenarios are shown in Figure 2. Global annual population exposure increases the most under RCP8.5-SSP3 and the least under RCP2.6-SSP1, with exposure being 1.41-fold (2016–2035) and 1.54-fold (2046–2065) higher than during the base period (Table S2). The growth of population exposure is highest in central and southeastern Africa, with the increases under the three RCP scenarios and the two periods exceeding 120%. The increases in exposure are also quite rapid for southern Asia, northwestern South America, and western North America under RCP4.5 and RCP8.5 and for eastern Oceania for 2046–2065. The increases relative to the base period are >60% in most of these regions. The increases are <60% in areas that typically have high population exposures such as China, western Europe, and eastern USA.

The relative changes in GDP exposure under the projected scenarios are shown in Figure 3. Global annual GDP exposure increases the most under the RC2.6-SSP1 scenario, followed by RCP4.5-SSP2 and RCP8.5-SSP3. Continental exposure is projected to increase the most in Africa, with an 8.70-fold increase relative to the base period, and increases the least in North America, with only a 1.35-fold increase relative to the base period. The GDP exposure for 2046–2065 increases significantly relative to both the base period and 2016–2035. For the spatial pattern, the increases in exposure are largest in eastern and southern Asia and central and southeastern Africa, all of which increase 8-fold relative to the base period. The GDP exposure also increases in northwestern and southeastern South America, southern Africa, and central and eastern Europe.

3.3. Analysis of the relative importance of factors affecting global population and GDP exposure at global and continental-scales

The changes in global population and GDP exposure and its components are shown in Figure 4. The changes in global population exposure are mainly due to the effect of population in all scenarios and time periods (64–77%), followed by the effects of climate (11–24%), with a small effect due to their interactions (5–11%) (Figure 4a). Population change for 2016–2035 accounts for >70% of the total change in exposure under the three scenarios, more than for 2046–2065. The change in GDP is the primary contributor (78–91%) to the total change of GDP exposure, followed by interactive (6–16%) and climatic (2–6%) effects for each scenario and period. The relative importance of the GDP effect decreases slowly for 2046–2065, and the contribution of the effects of climate and interactions is higher for 2046–2065 than 2016–2035. These results

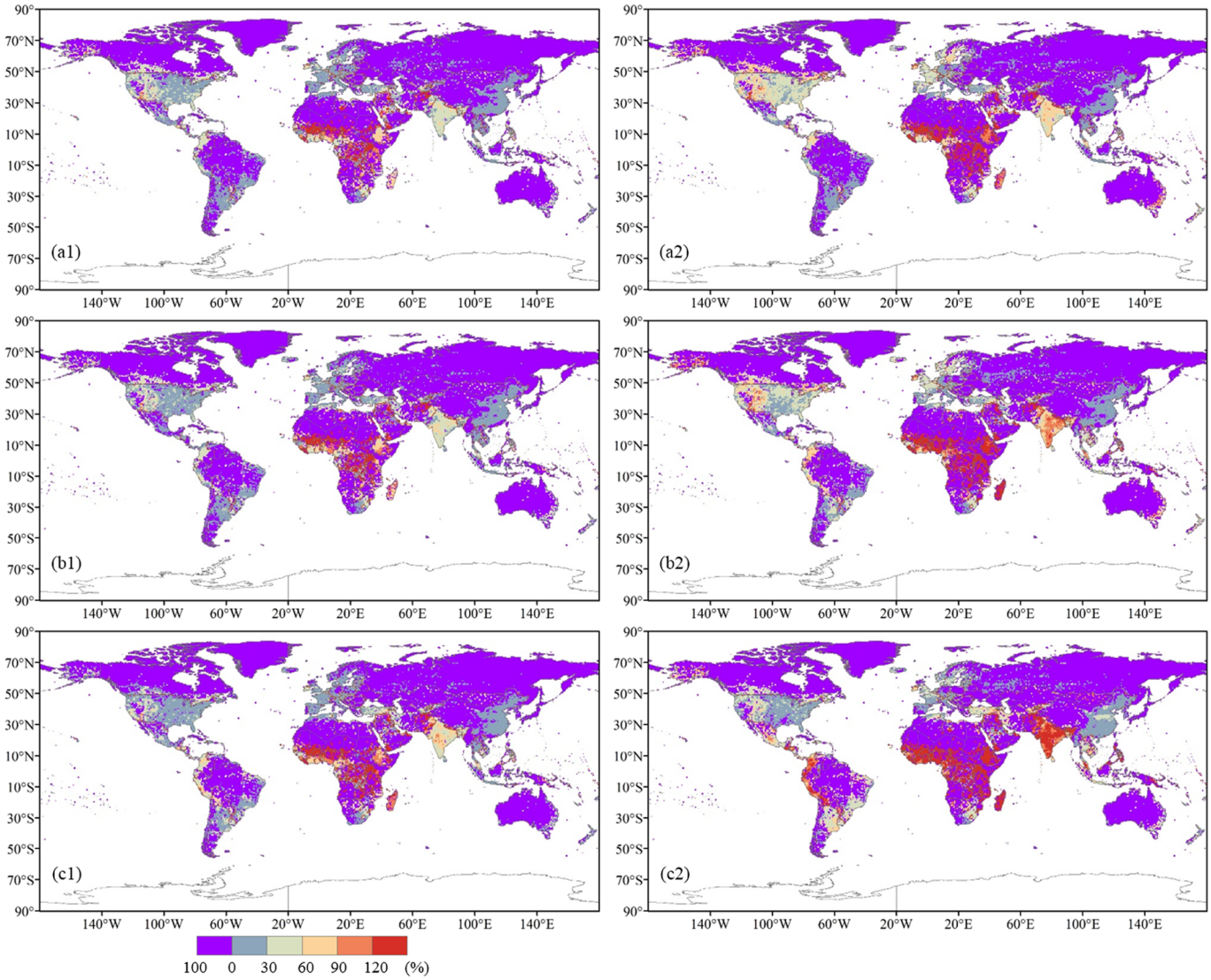

Figure 2. Spatiotemporal distribution of the multimodel average projected relative change of global population exposure relative to the base period for (a) RCP2.6-SSP1, (b) RCP4.5-SSP2, and (c) RCP8.5-SSP3, where (1) is 2016–2035 and (2) is 2046–2065.

indicate that the effect of climate would play a more important role in the total change in exposure over time, but that the effects of population and GDP would remain the dominant factors. The contribution of the GDP effect is highest under the RCP2.6-SSP1 and lowest under the RCP8.5-SSP3 scenario, because GDP growth is likely to slow in the pathways with higher GHG emissions.

The contribution of factors affecting the continental changes in population exposure (Figure 5) varies among the regions. For example, except for Europe, the change in exposure among continents is primarily affected by population change under all scenarios and in all periods. In Europe, the climate effect plays a more important role due to the slow population growth. There are also some differences among the other five continents. The relative importance of the various factors in Africa follows the order of population change > interactive change > climate change, with population change accounting for most (>75%) of the changes in exposure under all scenarios. In Asia, North America, South America, and Oceania, the effect of climate is more important than the effect of interactions in the changes in exposure. The effect of climate in Asia accounts for >25% of the change in exposure for 2016–2035, which increases to >35% for 2046–2065. Population change in South America and Oceania accounts for most of the total population change, at >90 and >80%, respectively.

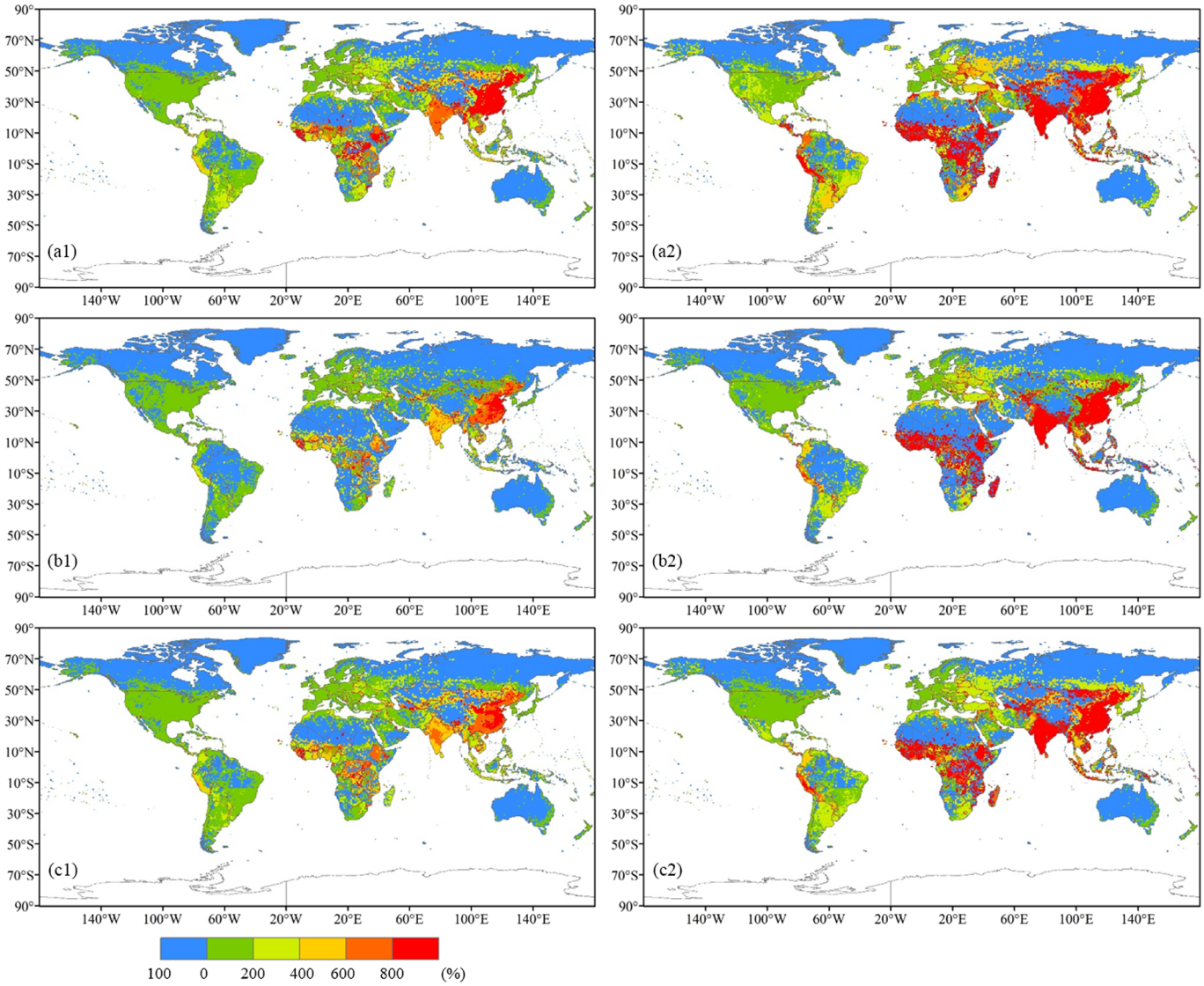

Figure 3. Spatiotemporal distribution of the multimodel average projected relative change of exposure of global gross domestic product (GDP) relative to the base period for (a) RCP2.6-SSP1, (b) RCP4.5-SSP2, and (c) RCP8.5-SSP3, where (1) is 2016–2035 and (2) is 2046–2065.

The contributions of the effects of GDP, climate, and their interactions to the continental changes in GDP exposure (Figure 6) differ among the continents, scenarios, and periods. In all continents, the effect of GDP is the primary contributor under each scenario and in each period. For example, the effect of GDP in South America accounts for >90% of the change in exposure under each scenario and in each period. The effect of GDP also accounts for >90% in Africa, except for 2046–2065 under the RCP8.5-SSP3 scenario (88%). The effect of GDP in Asia under all three scenarios accounts for >90% of the change in exposure for 2016–2035 and >75% for 2046–2065. The effects of climate and interactions are largest for 2046–2065 in the RCP8.5-SSP3 scenario (accounting for 16% and 17% of the changes in exposure, respectively). Climate change in Oceania for 2016–2035 in all three scenarios contributed to a decrease in GDP exposure, and the impact could be attributed to the less frequent extreme precipitation in 2016–2035 compared to the base period.

3.4. Inequality of nationally aggregated and united areas of population and GDP exposure

Climate change will increase inequality among future populations and GDP differences among countries, which may alter the amount of climate induced damage beyond that predicted from the global averaged

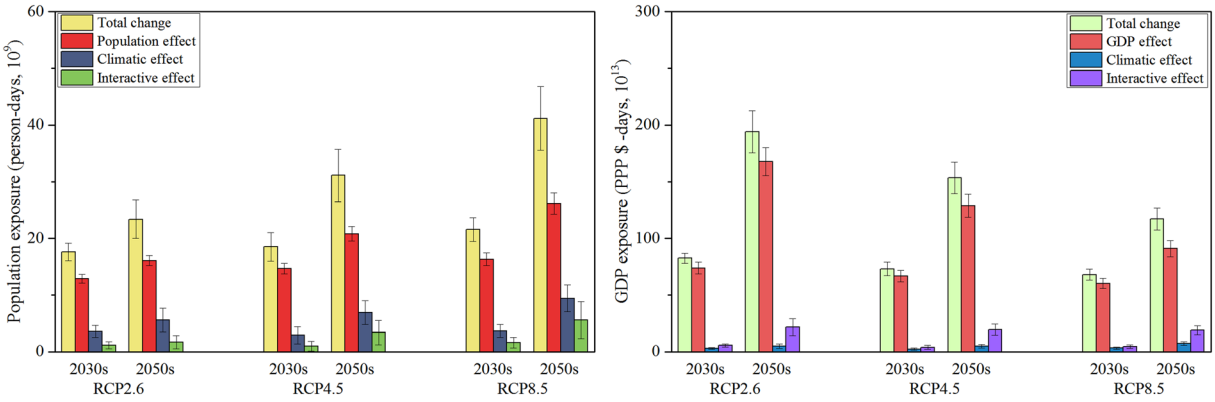

Figure 4. Decomposition of the changes in exposure of (a) global population and (b) gross domestic product (GDP) under the three scenarios (RCP2.6-SSP1, RCP4.5-SSP2, and RCP8.5-SSP3) and two time periods (2016–2035 and 2046–2065). Error bars indicate the standard deviations of the multimodel projections. PPP refers to purchasing-power parity and $ refers to US dollars.

expected exposure to climatic extremes. The inequality of nationally aggregated and united areas of population and GDP exposure in the scenarios with the highest exposures, that is, 2046–2065 in the RCP8.5-SSP3 scenario and 2046–2065 in the RCP2.6-SSP1 scenario. There are 189 countries whose exposures exceeded 0. The top 10 countries ordered by the nationally aggregated population and GDP

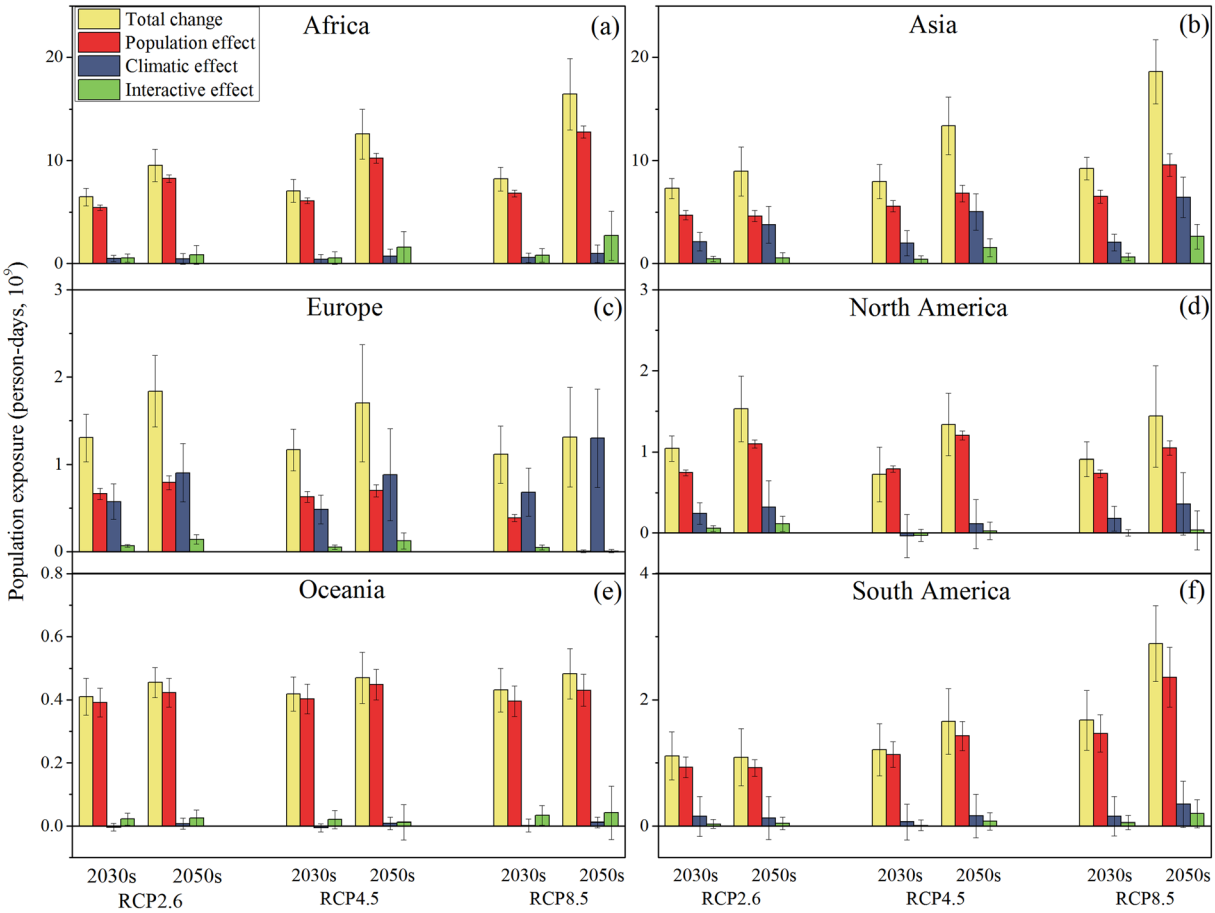

Figure 5. Decomposition of changes in continental population exposure under the three scenarios (RCP2.6-SSP1, RCP4.5-SSP2, and RCP8.5-SSP3) and two time periods (2016–2035 and 2046–2065) for (a) Africa, (b) Asia, (c) Europe, (d) North America, (e) Oceania, and (f) South America. Error bars indicate the standard deviations of the multimodel projections.

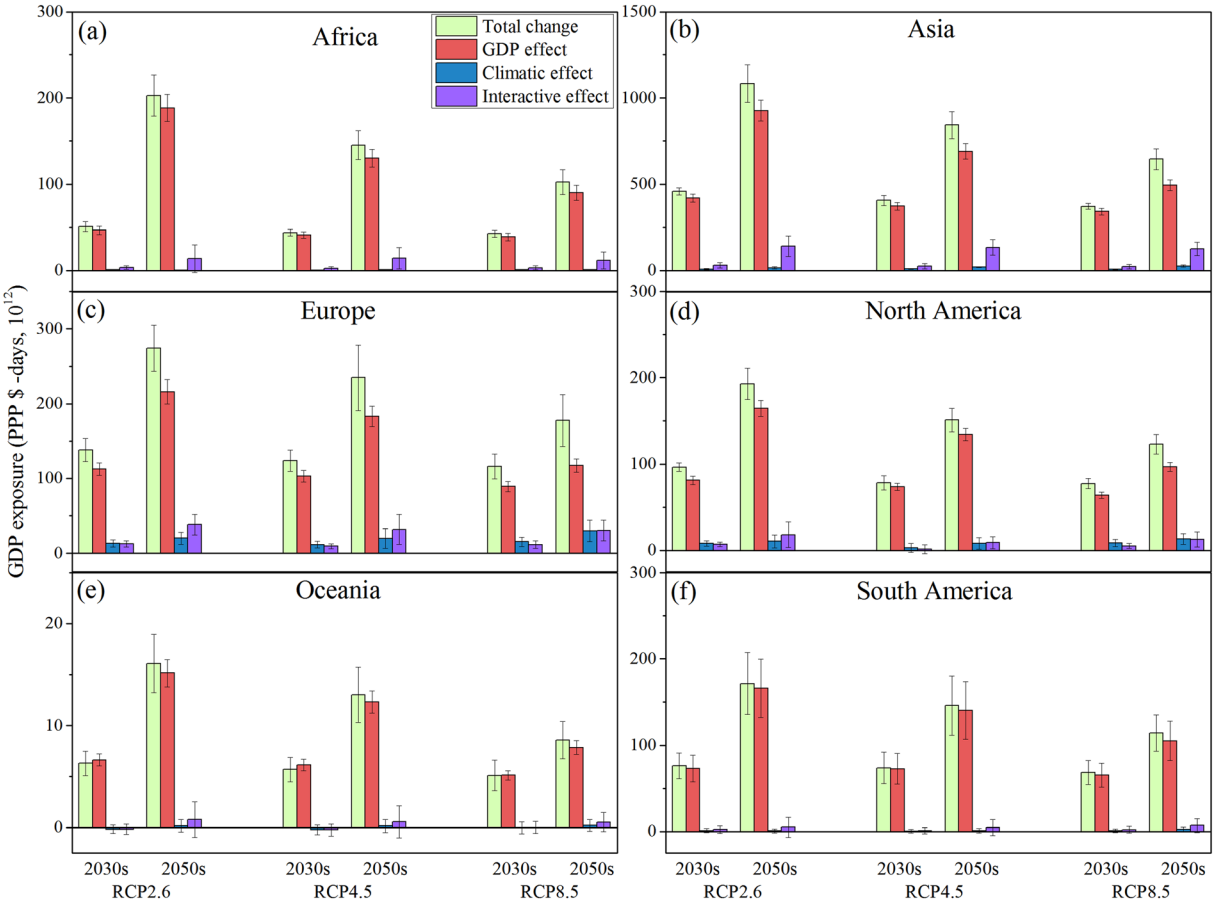

Figure 6. Decomposition of the change in exposure of continental gross domestic product (GDP) under the three scenarios (RCP2.6-SSP1, RCP4.5-SSP2, and RCP8.5-SSP3) and two time periods (2016–2035 and 2046–2065) in (a) Africa, (b) Asia, (c) Europe, (d) North America, (e) Oceania, and (f) South America. Error bars indicate the standard deviations of the multimodel projections. PPP refers to purchasing-power parity and $ refers to US dollars.

exposure in the two scenarios are shown in Figure 7. The results are expressed as the percentage of the total global exposure accounted for by the population and GDP exposure of each country. The 10 countries with the largest combined population and GDP exposure (population and GDP exposure density) are shown in Table 2.

The total exposures are much higher in countries with larger populations and GDP values. The 10 countries with the highest population exposures account for 53% of the global population exposure, with five of these countries in Asia and three in Africa. The top 20 countries account for 66% of the global exposure, with seven countries in each of Asia and Africa, and two each in Europe, North America, and South America. The 20 countries with the lowest population exposures account for only 2% of the total global exposure. These differences among countries are larger for the total GDP exposure. The 10 countries with the highest GDP exposures account for 66% of the global GDP exposure, with four countries in Asia and three in Europe. China has the highest exposure among all countries, accounting for 22% of the global GDP exposure. The top 20 countries account for 75% of the global exposure, with eight countries in Asia, five in Europe, and three each in North America and South America. The 20 countries with the lowest GDP exposures account for only 0.03% of the global exposure.

The inequalities of national population and GDP exposure density are large, and their distribution differs from that of total exposure. The top 10 countries with the highest population and GDP exposure density are shown in Table 2. The top 10 countries include four in Africa, three in Western Europe, and two in Asia. The annual population exposure in the three countries with the highest population exposures exceeds 1 million person-days/km^2. Europe accounts for six of the 10 countries with the highest GDP exposure

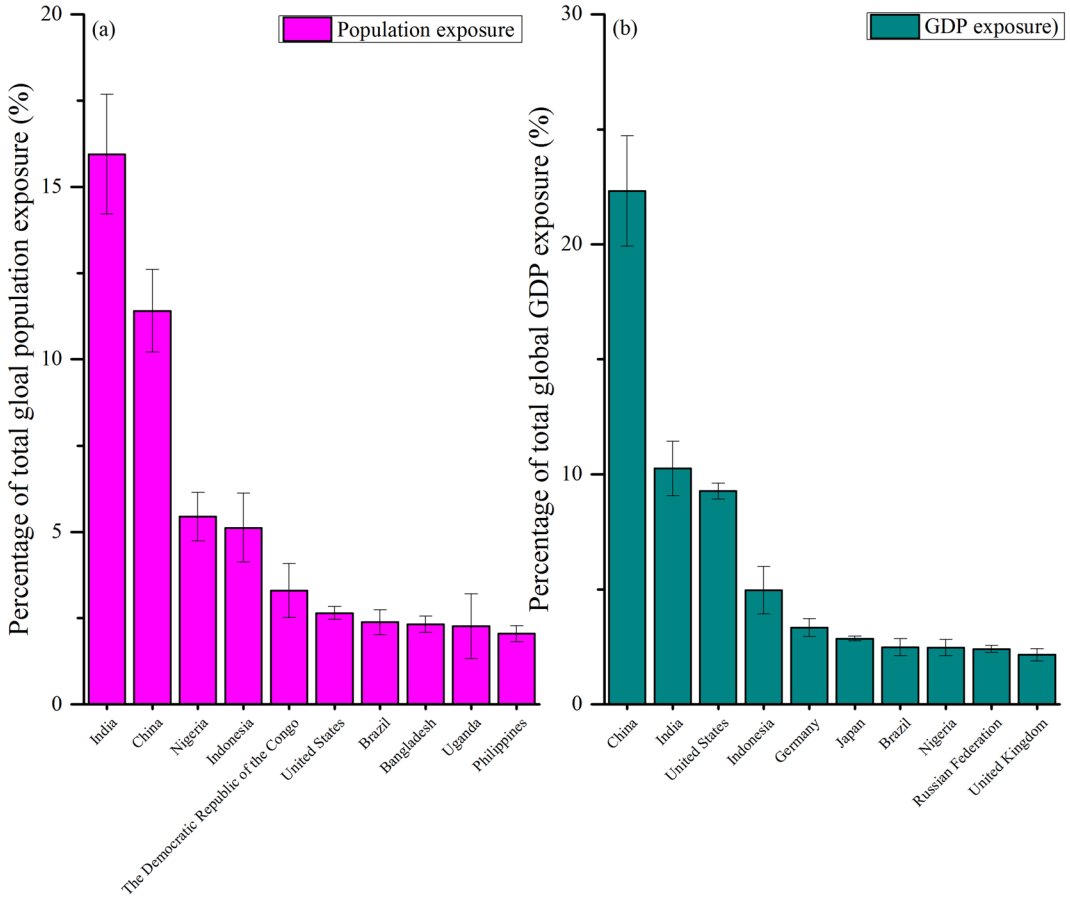

Figure 7. Inequality of (a) national population exposure under the RCP8.5-SSP3 scenario and (b) gross domestic product (GDP) exposure under the RCP2.6-SSP1 scenario in 189 countries whose exposure exceeded 0, ordered by the nationally aggregated population and GDP exposure under the corresponding scenario. The different colors indicate the values for different countries. Error bars indicate the standard deviations for the multimodel projections. PPP refers to purchasing-power parity and $ refers to US dollars.

density (Luxembourg, Belgium, the Netherlands, Switzerland, Germany, and the United Kingdom), while two countries are in Asia (South Korea and Japan). These countries are all developed countries, with a small geographical area, and therefore, their exposures are much higher than for other countries. The annual GDP exposures in the three countries with the highest population exposures are >30 million PPP dollar-days/km^2. This inequality of exposure among countries highlights a critical need for future research.

Table 2
The 10 Countries With the Largest National Populations and Highest GDP Exposure Densities

Country	Population exposure density (10^3 person-days/km^2)	Country	GDP exposure density (10^6 PPP $-days/km^2)
Rwanda	1871.25	Luxembourg	63.13
Burundi	1416.77	Belgium	46.78
Bangladesh	1250.95	The Netherlands	31.15
Uganda	746.16	South Korea	23.52
Belgium	689.95	Switzerland	22.28
Luxembourg	657.36	Germany	19.24
Philippines	544.26	Mauritius	18.67
Haiti	497.44	United Kingdom	18.12
Nigeria	469.02	Japan	15.53
The Netherlands	444.83	Bangladesh	14.21

4. Discussion

Existing estimates of socioeconomic exposure to climate extremes have typically been made on a regional basis, and there has been little consideration of population and GDP changes in the assessment of changes in exposure to climate extremes. Little information regarding the spatiotemporal variation of global socioeconomic exposure to extreme precipitation under different scenarios and time periods in a warmer future is available. Our findings fill these research gaps by quantifying the global population and GDP exposures to extreme precipitation in the RCP2.6-SSP1, RCP4.5-SSP2, and RCP8.5-SSP3 scenarios in two time periods (2016–2036 and 2046–2065). This analysis of the relative importance of different factors and an inequality analysis has quantified the impacts of different factors on exposure changes and identified the regions in need of effective adaptation. The results of our study will encourage further research on the internal mechanisms controlling the interactions among climate change, surface cover, and social activities. The results also provide a scientific basis for reducing the risk of extreme precipitation and ensuring sustainable socioeconomic development.

The assessment of population exposures under different scenarios and time periods demonstrates the importance of reducing GHG emissions. Annual global population exposure changes between the base period and 2046–2065 by about 53% increase (RCP2.6-SSP1), 71% increase (RCP4.5-SSP2), and 94% increase (RCP8.5-SSP3). Population exposure is highest under the RCP8.5 scenario, with rapid growth in both the population and the frequency of precipitation extremes. This result is consistent with those of previous studies of climatic extremes affecting human society (Cook et al., 2015; Harrington & Otto, 2018). The annual global GDP exposure increases between the base period and 2046–2065 by about 5.56-fold (RCP2.6-SSP1), 4.39-fold (RCP4.5-SSP2), and 3.35-fold (RCP8.5-SSP3). The GDP exposure is highest under the RCP2.6-SSP1 scenario, in which sustainable development proceeds moderately quickly, technological change is rapid (including reductions in fossil fuel energy sources), land productivity is high, and GDP growth is rapid (O'Neill et al., 2014). This increase in global population and GDP exposure is mainly due to the increased exposure in Asia and Africa, where both the population and GDP are projected to increase rapidly. However, this study is also subject to some limitations. First, for each RCP, it is likely that one or more SSP could lead to that climate path (IPCC, 2014). In this study, we selected the most consistently and widely used RCP-SSP combinations for which projected data were available. However, other combinations (e.g., RCP8.5-SSP5) are also likely to arise in the future. Perhaps not surprisingly, using different combinations may lead to alternative results. Thus, further studies using more different RCP-SSP combinations should be conducted when more data are available to decrease the uncertainty of the current results. Second, the frequency of extreme precipitation globally was computed using climate data from five GCMs that were spatially downscaled to $0.5° \times 0.5°$ resolution, due to the lack of higher resolution data at the global scale. Although the downscaled data have been proved to preserve relative changes in monthly values of precipitation in each grid cell and imply the global warming trend, the relatively coarse resolution of the original GCMs is likely to cause deviations in the predictions of future occurrences of precipitation extremes. Thus, further studies could evaluate changes in global precipitation extremes as well as their impact on socioeconomic systems under climate change using more sophisticated data with higher resolution, and generate assessment results that are more accurate and reasonable.

The analysis of the relative importance of factors at global and continental scales indicates that the effects of population and GDP are the primary contributors to the changes in exposure globally, and on all continents except Europe, where the effect of climate is the main contributor to the change in population exposure. The effect of climate has an increasingly important role in the total change in exposure over time, but the effects of population and GDP remain the dominant factors. Increases in exposure are primarily due to rapidly increasing populations and large increases in GDP. This result is similar to that of Winsemius et al. (2016), who determined the future global risk of river flooding, and revealed a large increase in risk in southeastern Asia and Africa due mainly to socioeconomic changes. Populations are expected to adapt to climate change in numerous ways, such as establishing safer living conditions, adjusting crop varieties and planting conditions, and building higher dams (Davis & Gertler, 2015; Schlenker et al., 2013); therefore, exposure may not necessarily lead to demographic and economic losses. Wealthy populations are expected to adapt to climate change more effectively with future rapid GDP growth due to their greater resources, wider arrays of technology, and stronger governments (Kahn, 2005; Lomborg, 2004). However, potential constraints in the implementation of future adaptive measures may lead to inadequate adaptation. These constraints

include very high costs (Guo et al., 2014), limited benefits (Hornbeck, 2012), a lack of clarity of the purpose of adaptation (Hsiang & Narita, 2012), weak management by governments (Besley & Burgess, 2002), and insufficient funding (Annan & Schlenker, 2015). The design and implementation of effective adaptive measures are therefore urgently needed for populations suffering from precipitation extremes and to reduce the economic losses under climate change.

The inequality of exposure analysis reveals that the highest exposures are projected to occur in Asia and Africa. The inequality of exposure at continental and national scales is obvious (Figures S2 and S3). Population exposure in Asia accounts for >50% of the global exposure (Table S2), with Africa having the second highest continental exposure. The proportional population exposure in Asia and Africa is projected to increase over time with the continuing emission of GHGs. These two continents account for 75% of the global population exposure under the RCP8.5-SSP3 scenario. Asia accounts for almost 50% of the global exposure in the future scenarios for continental GDP exposure (Table S3), followed by Europe and North America. These three continents account for >80% of the global GDP exposure. The three countries with both the highest nationally aggregated population and GDP exposures are in Asia and include China, India, and Indonesia. Developed countries in western Europe, that is, Luxembourg, Belgium, and the Netherlands, are among the 10 countries with both the highest population and GDP exposures density. The influence of the inequality of climate change on the socioeconomic system has previously been reported. For example, Hsiang et al. (2017) reported that economic losses in United States will be distributed unequally across areas under climate change, leading to increasing economic inequality in the country. There is an unequal distribution of exposure at the global scale, with pronounced variation among regions. These findings indicate that more attention should be given to Asia and Africa due to their rapid increases in population and GDP. However, Europe should also commit to effective adaptation measures because it has many countries with dense populations and large GDPs, leading to higher exposures than other areas of the world.

5. Conclusions

This study achieved four key findings. First, global population exposure is highest under the RCP8.5-SSP3 scenario, with the exposure for 2046–2065 increasing 0.94-fold relative to the base period, and nearly 30% of global population (2.97×10^9 persons) exposed to precipitation extremes of >10 days per year. Global GDP exposure is highest under the RCP2.6-SSP1 scenario for 2046–2065, with exposure increasing 5.56-fold relative to the base period. Second, the increases in global population and GDP exposures are mainly due to the increased exposures in Asia and Africa. Both population and GDP exposure are highest in Asia, which accounts for nearly 50% of the global exposure under each RCP scenario, with the largest increase in exposure occurring in Africa. Third, socioeconomic effects (population and GDP) rather than the effect of climate are the primary contributors to changes in exposure at global and continental scales under climate change, except in Europe. Fourth, the inequality of exposure at continental and national scales indicates that more attention should be given to Asia and Africa due to their rapid increases in population and GDP. However, European countries should also commit to effective adaptation measures due to their dense populations and high GDPs. Our findings demonstrate the importance of mitigating GHG emissions to reduce socioeconomic exposure to extreme precipitation. There is an urgent need to design and implement effective adaptive measures to enable socioeconomic systems to overcome precipitation extremes.

Acknowledgments

This study was supported by the National Key Research and Development Program of China (grant no. 2016YFA0602402), the National Natural Science Foundation of China (grant no. 41671037), the Youth Innovation Promotion Association, Chinese Academy of Sciences (CAS) (grant no. 2016049), and the Program for "Kezhen" Excellent Talents in the Institute of Geographic Sciences and Natural Resources Research (IGSNRR), (grant no. 2017RC101). Funding for JP's research was provided by the European Research Council Synergy grant ERC-SyG-2013-610028 IMBALANCE-P. We also thank ISI-MIP and NIES for providing data support. The precipitation data used in the RCP scenarios are available online (https://www.isimip.org/getting-started/#input-data-bias-correction). The population and GDP data used in the SSP scenarios are available online (http://www.cger.nies.go.jp/gcp/population-and-gdp.html).

References

Annan, F., & Schlenker, W. (2015). Federal Crop Insurance and the Disincentive to Adapt to Extreme Heat. *American Economic Review*, *105*(5), 262–266. https://doi.org/10.1257/aer.p20151031

Besley, T. J., & Burgess, R. (2002). The Political Economy of Government Responsiveness: Theory and Evidence from India. *SSRN Electronic Journal*. https://doi.org/10.2139/ssrn.319012

Bouwer, L. M. (2013). Projections of future extreme weather losses under changes in climate and exposure. *Risk Analysis An Official Publication of the Society for Risk Analysis*, *33*, 915–930. https://doi.org/10.1111/j.1539-6924.2012.01880.x

Bowles, D. C., Butler, C. D., & Friel, S. (2014). Climate change and health in Earth's future. *Earths Future*, *2*, 60–67. https://doi.org/10.1002/2013EF000177

Carleton, T. A., & Hsiang, S. M. (2016). Social and economic impacts of climate. *Science*, *353*, aad9837. https://doi.org/10.1126/science.aad9837

Ceola, S., Laio, F., & Montanari, A. (2015). Satellite nighttime lights reveal increasing human exposure to floods worldwide. *Geophysical Research Letters*, *41*, 7184–7190. https://doi.org/10.1002/2014GL061859

Cook, B. I., Ault, T. R., & Smerdon, J. E. (2015). Unprecedented 21st century drought risk in the American Southwest and Central Plains. *Science Advances*, *1*, e1400082. https://doi.org/10.1126/sciadv.1400082

Davis, L. W., & Gertler, P. J. (2015). Contribution of air conditioning adoption to future energy use under global warming. *Proceedings of the National Academy of Sciences of the United States of America*, *112*, 5962–5967. https://doi.org/10.1073/pnas.1423558112

Forzieri, G., Cescatti, A., Silva, F. B. E., & Feyen, L. (2017). Increasing risk over time of weather-related hazards to the European population: A data-driven prognostic study. *The Lancet Planetary Health*, *1*, e200–e208. https://doi.org/10.1016/s2542-5196(17)30082-7

Giorgi, F., Im, E. S., Coppola, E., Diffenbaugh, N. S., Gao, X. J., Mariotti, L., & Shi, Y. (2011). Higher hydroclimatic intensity with global warming. *Journal of Climate*, *24*(20), 5309–5324. https://doi.org/10.1175/2011jcli3979.1

Groisman, P. Y., Karl, T. R., Easterling, D. R., Knight, R. W., Jamason, P. F., Hennessy, K. J., et al. (1999). Changes in the Probability of heavy precipitation: Important indicators of climatic change. *Climatic Change*, *42*(1), 243–283. https://doi.org/10.1007/978-94-015-9265-9_15

Guo, Y., Gasparrini, A., Armstrong, B., Li, S., Tawatsupa, B., Tobias, A., et al. (2014). Global variation in the effects of ambient temperature on mortality: A systematic evaluation. *Epidemiology*, *25*(6), 781–789. https://doi.org/10.1097/ede.0000000000000165

Harrington, L. J., & Otto, F. E. L. (2018). Changing population dynamics and uneven temperature emergence combine to exacerbate regional exposure to heat extremes under 1.5°C and 2°C of warming. *Environmental Research Letters*, *13*, 034011. https://doi.org/10.1088/1748-9326/aaaa99

Hempel, S., Frieler, K., Warszawski, L., Schewe, J., & Piontek, F. (2013). A trend-preserving bias correction—The ISI-MIP approach. *Earth System Dynamics*, *4*, 219–236. https://doi.org/10.5194/esd-4-219-2013

Hornbeck, R. (2012). The enduring impact of the American dust bowl: Short- and long-run adjustments to environmental catastrophe. *American Economic Review*, *102*(4), 1477–1507. https://doi.org/10.1257/aer.102.4.1477

Houser, T., Hsiang, S., Kopp, R., Larsen, K., Delgado, M., Jina, A., et al. (2015). *Economic risks of climate change: An American prospectus*. Columbia, USA: Columbia University Press. https://doi.org/10.7312/hous17456

Hsiang, S., Kopp, R., Jina, A., Rising, J., Delgado, M., Mohan, S., et al. (2017). Estimating economic damage from climate change in the United States. *Science*, *356*, 1362–1369. https://doi.org/10.1126/science.aal4369

Hsiang, S. M., & Narita, D. (2012). Adaptation to cyclone risk: evidence from the global cross-section. *Climate Change Economics*, *03*(02), 1250011. https://doi.org/10.1142/s201000781250011x

IPCC (2012). *Managing the risks of extreme events and disasters to advance climate change adaptation: Special report of the intergovernmental panel on climate change*. Cambridge, UK, New York, NY: Cambridge University Press.

IPCC (2013). Climate change 2013: The physical science basis. In *Contribution of working group I to the fifth assessment report of the intergovernmental panel on climate change* (pp. 1–1535). Cambridge, UK, New York, NY: Cambridge University Press.

IPCC (2014). Climate change 2014: Impacts, adaptation, and vulnerability. Part A: Global and 248 Sectoral Aspects. In *Contribution of working group II to the fifth assessment report of the 249 intergovernmental panel on climate change* (pp. 1–1132). Cambridge, UK, New York, NY: Cambridge University Press.

Jones, B., O'Neill, B. C., Mcdaniel, L., Mcginnis, S., Mearns, L. O., & Tebaldi, C. (2015). Future population exposure to US heat extremes. *Nature Climate Change*, *5*, 652–655. https://doi.org/10.1038/nclimate2631

Kahn, M. E. (2005). The death toll from natural disasters: The role of income, geography, and institutions. *Review of Economics & Statistics*, *87*(2), 271–284. https://doi.org/10.2139/ssrn.391741

Kharin, V. V., Zwiers, F. W., Zhang, X., & Wehner, M. (2013). Changes in temperature and precipitation extremes in the CMIP5 ensemble. *Climatic Change*, *119*, 345–357. https://doi.org/10.1007/s10584-013-0705-8

King, A. D., Donat, M. G., Lewis, S. C., Henley, B. J., Mitchell, D. M., Stott, P. A., et al. (2018). Reduced heat exposure by limiting global warming to 1.5°C. *Nature Climate Change*, *8*, 549–551. https://doi.org/10.1038/s41558-018-0191-0

King, A. D., Karoly, D. J., & Henley, B. J. (2017). Australian climate extremes at 1.5°C and 2°C of global warming. *Nature Climate Change*, *7*, 412–416. https://doi.org/10.1038/nclimate3296

Liu, J., Hertel, T. W., Diffenbaugh, N. S., Delgado, M. S., & Ashfaq, M. (2015). Future property damage from flooding: Sensitivities to economy and climate change. *Climatic Change*, *132*, 741–749. https://doi.org/10.1007/s10584-015-1478-z

Liu, Z., Anderson, B., Yan, K., Dong, W., Liao, H., & Shi, P. (2017). Global and regional changes in exposure to extreme heat and the relative contributions of climate and population change. *Scientific Reports*, *7*, 43909. https://doi.org/10.1038/srep43909

Lomborg, B. (2004). *Global crises, global solutions* (Vol. 330, pp. 222–223). Cambridge, USA: Cambridge University Press.

Min, S. K., Zhang, X., Zwiers, F. W., & Hegerl, G. C. (2011). Human contribution to more-intense precipitation extremes. *Nature*, *470*(7334), 378–381. https://doi.org/10.1038/nature09763

Mitchell, D., AchutaRao, K., Allen, M., Bethke, I., Beyerle, U., Ciavarella, A., et al. (2017). Half a degree additional warming, prognosis and projected impacts (HAPPI): Background and experimental design. *Geoscientific Model Development*, *10*, 571–583. https://doi.org/10.5194/gmd-10-571-2017

Murakami, D., & Yamagata, Y. (2019). Estimation of gridded population and GDP scenarios with spatially explicit statistical downscaling. *Sustainability*, *11*, 2106. https://doi.org/10.3390/su11072106

O'Neill, B. C., Kriegler, E., Ebi, K. L., Kemp-Benedict, E., Riahi, K., Rothman, D. S., et al. (2017). The roads ahead: Narratives for shared socioeconomic pathways describing world futures in the 21st century. *Global Environmental Change*, *42*, 169–180. https://doi.org/10.1016/j.gloenvcha.2015.01.004

O'Neill, B. C., Kriegler, E., Riahi, K., Ebi, K. L., Hallegatte, S., Carter, T. R., et al. (2014). A new scenario framework for climate change research: The concept of shared socioeconomic pathways. *Climatic Change*, *122*, 401–414. https://doi.org/10.1007/s10584-013-0905-2

Pryor, S. C., Scavia, D., Downer, C., Gaden, M., Iverson, L., Nordstrom, R., et al. (2014). Midwest. Climate change impacts in the United States: The third national climate assessment. In *National Climate Assessment Report* (pp. 418–440). Washington, DC: US Global Change Research Program.

Schlenker, W., Roberts, M. J., & Lobell, D. B. (2013). US maize adaptability. *Nature Climate Change*, *3*, 690–691. https://doi.org/10.1038/nclimate1959

Smirnov, O., Zhang, M., Xiao, T., Orbell, J., Lobben, A., & Gordon, J. (2016). The relative importance of climate change and population growth for exposure to future extreme droughts. *Climatic Change*, *138*, 41–53. https://doi.org/10.1007/s10584-016-1716-z

Sun, H., Wang, Y., Chen, J., Zhai, J., Jing, C., Zeng, X., et al. (2017). Exposure of population to droughts in the Haihe River Basin under global warming of 1.5 and 2.0 °C scenarios. *Quaternary International*, *453*, 74–84. https://doi.org/10.1016/j.quaint.2017.05.005

Taylor, K. E., Stouffer, R. J., & Meehl, G. A. (2012). An overview of CMIP5 and the experiment design. *Bulletin of the American Meteorological Society*, *93*(4), 485–498. https://doi.org/10.1175/BAMS-D-11-00094.1

Toreti, A., Naveau, P., Zampieri, M., Schindler, A., Scoccimarro, E., Xoplaki, E., et al. (2013). Projections of global changes in precipitation extremes from coupled model intercomparison project phase 5 models. *Geophysical Research Letters*, *40*, 4887–4892. https://doi.org/10.1002/grl.50940

Van Vuuren, D. P., & Carter, T. R. (2014). Climate and socio-economic scenarios for climate change research and assessment: Reconciling the new with the old. *Climatic Change*, *122*, 415–429. https://doi.org/10.1007/s10584-013-0974-2

Vuuren, D. P. V., Edmonds, J., Kainuma, M., Riahi, K., Thomson, A., Hibbard, K., et al. (2011). The representative concentration pathways: An overview. *Climatic Change*, *109*(1-2), 5–31. https://doi.org/10.1007/s10584-011-0148-z

Vuuren, D. P. V., Edmonds, J. A., Kainuma, M., Riahi, K., & Weyant, J. (2011). A special issue on the RCPs. *Climatic Change*, *109*(1-2), 1–4. https://doi.org/10.1007/s10584-011-0157-y

Warszawski, L., Frieler, K., Huber, V., Piontek, F., Serdeczny, O., & Schewe, J. (2014). The inter-sectoral impact model intercomparison project (ISI-MIP): Project framework. *Proceedings of the National Academy of Sciences of the United States of America*, *111*, 3228–3232. https://doi.org/10.1073/pnas.1312330110

Westra, S., Fowler, H. J., Evans, J. P., Alexander, L. V., Berg, P., Johnson, F., et al. (2014). Future changes to the intensity and frequency of short-duration extreme rainfall. *Reviews of Geophysics*, *52*, 522–555. https://doi.org/10.1002/2014RG000464

Winsemius, H. C., Aerts, J. C. J. H., van Beek, L. P. H., Bierkens, M. F. P., Bouwman, A., Jongman, B., et al. (2016). Global drivers of future river flood risk. *Nature Climate Change*, *6*, 381–385. https://doi.org/10.1038/nclimate2893

WMO (2010). Report of the meeting of the management group of the commission for climatology. Geneva, 18-21 May, 2010.

WMO (2020). WMO statement on the state of the global climate in 2019. https://library.wmo.int/doc_num.php?explnum_id=10211

Zhang, W., Zhou, T., Zou, L., Zhang, L., & Chen, X. (2018). Reduced exposure to extreme precipitation from 0.5 °C less warming in global land monsoon regions. *Nature Communications*, *9*, 3153. https://doi.org/10.1038/s41467-018-05633-3